Prediction of FDG-PET stage and uptake for non-small cell lung cancer on non-contrast enhanced CT scans via fractal analysis

Omar Al-Kadi

University of Jordan, Amman 11942 Jordan

Abstract

Purpose: To investigate whether the FD of non-small cell lung cancer (NSCLC) on CT predicts tumor stage and uptake on ^{18}F-fluorodeoxyglucose positron emission tomography.

Material and Methods: The FD within a tumor region was determined using a box counting algorithm and compared to the lymph node involvement (NI) and metastatic involvement (MI) and overall stage as determined from PET. A Mann-Whitney U test was applied to the extracted FD features for the NI and the MI.

Results: The two tests showed good significance with $p < 0.05$ ($p_{NI} = 0.0139$, $p_{MI} = 0.0194$). Also after performing fractal analysis to all cases, it was found that for those who had a CT of stage I or II had a higher likelihood of the NI and/or MI stage being upstaged by PET, Odds Ratio 5.38 (95% CI 0.99 -29.3). For those who are CT stage III or IV had an increased likelihood of the NI and/or MI stage being down staged by PET, Odds Ratio: 7.33 (95% CI 0.48 -111.2).

Conclusion: Initial results of this study indicate higher FD in CT images of NSCLC is associated with advanced stage and greater FDG uptake on PET. Measurements of tumor fractal analysis on conventional non-contrast CT examinations could potentially be used as a prognostic marker and/or to select patients for PET.

Keywords: Fractal dimension, fractal analysis, computed tomography, positron emission tomography, non-small cell carcinomas

1. Introduction

The healthcare burden and economical costs associated with lung cancer is substantial on a global scale [1]. It is the most common cause of cancer death, where about 55% of the reported cases occurred in the developing countries and nearly one in five of all cancer deaths in the developed countries are from lung cancer [2, 3].

The prognosis and management of lung cancer depends on the patient's physical condition, the histopathology of the tumor and the disease extent. The 3-year cumulative survival for non-small cell lung cancer (NSCLC) was found to be for stage I 39%, stage II 30%, stage III 6% and stage IV 0.5% [4]. Lung cancers can be generally classified into two histological categories, non-small cell and small cell carcinomas. While small cell carcinomas, which account for 20–25% of all lung cancers, have already disseminated by time of presentation in 80% of cases NSCLCs that are localized or locally advanced at diagnosis, are treated by resection alone or with chemotherapy and radiotherapy [5].

Staging is mostly used for non-small cell carcinomas, where patients are staged so that management decisions can be made and then used to identify patients who will benefit from surgery. Current ways of clinical staging are through non-invasive assessments, which include the medical history, patient examination and laboratory tests Greene et al. [5]. Computed tomography (CT) is most commonly used in the staging of patients as it is widely available and can be readily interpreted. Positron emission tomography (PET) is used after CT in selected patients, but it is more expensive and there are a limited number of scanners.

The tumor node metastatic staging classification involves the intra-thoracic assessment of the primary tumor with its size, location, relationship to surrounding structures, the nodal involvement, and whether there has been systemic metastasis. The nodal status is an important factor to decide whether the patient qualifies for surgical treatment. CT and magnetic resonance imaging (MRI) assess the size of the lymph nodes while ^{18}F-fluorodeoxyglucose positron emission tomography (FDG-PET) assesses the metabolic activity. According to the National Institute for Health and Clinical Excellence (NICE) guidelines the sensitivity and specificity of CT in staging the nodal status is 57% (95 CI 49–66%) and 82% (95% CI 77–86%) respectively [6]. The

positive and negative predictive value was 56% (range 26–84%) and 83% (range 63–93%) respectively. From the above findings we can see that a significant number of patients (approximately 40–45%) with nodal disease are miss-classified. For FDG-PET the sensitivity and specificity was 84% (95 CI 0.78–0.89%), 89% (95% CI 0.83–0.93%), respectively, PPV 79% (range 0.4–1.0%), and NPV 93% (range 0.75–1.0%). In summary, FDG-PET has been shown to be more accurate in the determination of mediastinal nodal disease than CT [6]; therefore, improvements in CT performance would be useful.

Fractal analysis measures the complexity of a structure compared to the surrounding region. Therein, image intensities from CT scans are transformed to quantitative values assessing the irregularity or heterogeneity of the image texture surface – called fractal dimension (FD) – and then fractal analysis is performed. The transformation looks at the spatial variation in intensity of each pixel within a predefined local neighborhood. Irregularity in tumors has been associated with increased severity and thus stage, so this complexity may also be related to corresponding fractal dimension values [7]. Fractal analysis has been previously used to distinguish benign from malignant disease, and in the quantification of diffuse lung abnormality like idiopathic pulmonary fibrosis, ground glass opacities and also for the quantitative evaluation of pulmonary emphysema. Also it has been used for investigation of peripheral pulmonary nodules detected by high resolution CT. Previous work has shown the feasibility of the fractal dimension in analyzing and staging lung tumor texture regions acquired via contrast enhanced CT images [8], and was less susceptible to acquisition noise Al-Kadi [9]. Kido et al. tried to distinguish bronchogenic carcinomas from benign pulmonary nodules, and they concluded it may be possible to distinguish adenocarcinomas from squamous cell carcinomas Kido et al. [10]. In another similar work, fractal analysis was employed to differentiate pure bronchoalveolar carcinomas, which has a good prognosis from non-bronchoalveolar cell carcinoma Kido et al. [11]. Other works showed that there is a significant relationship between texture features in NSCLC on non-contrast-enhanced CT and tumor metabolism and stage Ganeshan et al. [12], and in another study the potential for tumor heterogeneity in NSCLC, as assessed by CT texture analysis, to provide an independent marker of survival for patients with NSCLC was investigated Ganeshan et al. [13].

In this context, studies which employed FDG-PET in NSCLC is the work by Borst et al, which investigated the relationship between standard-

ized FDG uptake value (SUV) obtained from FDG-PET and treatment response/survival of inoperable NSCLC patients treated with high dose radiotherapy Borst et al. [14]. Lee et al evaluated the response and survival for platinum-based combination chemotherapy in chemonaïve patients with NSCLC according to pretreatment standardized FDG-PET Lee et al. [15]. Mac Manus et al showed that the intensity of FDG uptake in pulmonary tissue after radiation therapy determined using a simple visual scoring system had a significant correlation with the presence and severity of radiation pneumonitis Mac Manus et al. [16]. Also de Geus-Oei et al evaluate the usefulness of FDG-PET for the assessment of chemotherapy response in patients with non-small cell lung cancer de Geus-Oei et al. [17]. The predictive capabilities of diffusion-weighted MRI and FDG-PET/CT for tumor response to therapy and survival in patients with NSCLC receiving chemoradiotherapy was compared by Ohno et al Ohno et al. [18], and Zhang et al evaluated FDG-PET/CT for the assessment of therapy response and prediction of patient outcome after concurrent chemoradiotherapy Zhang et al. [19]. A review on the different texture analysis methods applied in FDG PET/CT for providing predictive and prognostic information can be found in Chicklore et al. [20].

The aim of this paper is to investigate whether if the FD or complexity of the texture of a tumor correlates with PET findings and tumor stage. If we demonstrate that we are able to predict the likely PET findings and tumor stage from conventional non-contrast enhanced CT scans – which is considered more challenging as compared to contrast enhanced CT scans – this would improve selection of patients for PET scans.

2. Materials and Methods

2.1. Clinical data

Images of primary tumors were obtained from PET-CT studies in Brighton & Sussex University Hospitals NHS Trust (Brighton, UK) of 56 patients (31 males and 25 females with age 68 10 years old) diagnosed with NSCLC, between the period of April 2006 and November 2006 were included in the study. PET-CT was performed as these patients were considered potentially suitable for surgery or chemotherapy on the basis of an initial CT. Patients were grouped as stage I, II, III or IV using conventional CT criteria for tumor size and local invasion and PET assessments of nodal and distant metastases. Based on FDG-PET imaging, the number of patients with tumor stages I, II,

III and IV were 25, 12, 15 and 4 respectively. Average tumor SUV for all patients was 14.13 (3.2 - 34). Patients had fasted for six hours prior to the study and their height, weight and serum glucose level was recorded. Histological examination of biopsy material confirmed NSCLC in all patients. All clinical PET-CT examinations had been dual-reported by radiologists/nuclear medicine physicians. PET images were re-analyzed to obtain SUV_{max} measurements of FDG uptake by an operator blinded to the results of fractal analysis.

2.2. Image acquisition

A GE Discovery ST PET-CT system (GE Healthcare, Waukesha, WI, USA) modality was used, with both CT and PET data acquired in one procedure in accordance with a standardized protocol. PET-CT images had been acquired in the supine position 60 minutes after an injection of 400 MBq of ^{18}F-FDG. The CT acquisition comprised of an initial digitally acquired radiograph (10 mAs, 120 kVp, fixed rotational speed) followed by a conventional low-dose CT of the neck, chest abdomen and pelvis without contrast material (80 mAs, 140 kVp, rotational speed = 0.8 s/rot, pitch = 1.5, slice thickness = 3.75 mm). The pixel size for the non-enhanced CT images used in this study was 0.98 mm. To enable subsequent calculation of tracer uptake expressed as the standardized uptake value, the initial activity and time, administration time, and residual activity and time had been recorded.

2.3. Fractal Analysis

The FD within a tumor region was determined on a pixel-by-pixel basis using a box counting algorithm and compared to the nodal, metastatic and overall stage determined from PET. FD was also correlated with the maximal (SUV_{max}), which represents the pixel with the highest FDG tumor uptake activity, and average (SUV_{avg}), which represents the average of FDG tumor uptake activity in an area Adams et al. [21]. Fractals are used to describe non-Euclidean structures that show self-similarity at different scales as formulated in Equation (1) Al-Kadi [22], Mandelbrot [23]. Given that most biological and natural features show discontinuities and fragmentation so they tend to have a fractal dimension (FD).

$$FD = \frac{log(N_k)}{log(\frac{1}{k})} \tag{1}$$

Where N_k is the number of self-similar shapes and k is the corresponding scaling factor (i.e. the size of the scaling kernel around each pixel). Theoretically, the scaling factor k should represent how much a specific structure of pixels are self-similar to its surrounding. For the 512 mm 512 mm CT images having a resolution of 16 bits/pixel, the k range was chosen to be in the range between 2 to 7 and found that the best scaling is achieved in this range as the FD image starts to become blurry Al-Kadi and Watson [8], due to resolution constraints of the image, if we tend to extend the range deeper.

The differential box counting algorithm Li et al. [24], Chen et al. [25], Buczkowski et al. [26], Sarkar and Chaudhuri [27] was used to estimate the fractal dimension for each pixel in the CT image. The original CT image of size M N is transformed to a FD parametric image by applying a varying size non-linear kernel of m n as: $(a, b) = \mathsf{d}(k/2, k/2)\mathsf{e}$ for odd size kernels, and $(a, b) = \mathsf{d}(k/2 + 1, k/2 + 1)\mathsf{e}$ for even size kernels that operates by block processing on the neighboring pixels, where $k = 2, 3, 4, \ldots, j$ is the scaling factor, and the two variables a and b represent non-negative integers that center the kernel $n(s, t)$ on pixel p_{xy} in the original image. By varying k, we vary the size of the kernel bounding the pixel as illustrated in (Fig. 1). The kernel finds the difference between the highest (p_{max}) and lowest (p_{min}) intensity pixels and divides the results by the scaling factor as shown in (Fig. 2). Then the floor of the results is taken and one is added to make sure no zeros are encountered when we take the logarithm of all results. The kernel is applied as in Equation (2) giving the output image.

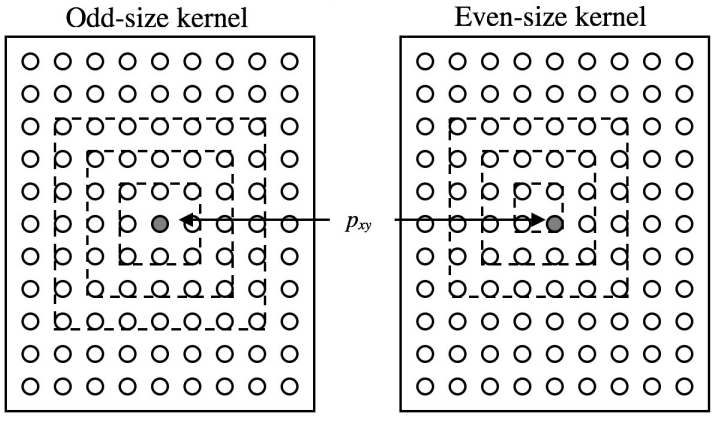

Figure 1: Odd and even size kernels applied to acquired CT image I, and p_{xy} is the pixel operated upon.

$$F(x,y) = \sum_{s=-a}^{a} \sum_{t=-b}^{b} n(s,t) I(x+s, y+t) \tag{2}$$

The output image $F(x,y)$ is then multiplied by the square of the highest scale value j and divided by the square of the relative scale of the applied kernel as shown in Equation (3).

$$N_d(x,y) = \left\lfloor \frac{F(x,y) \quad j^2}{k^2} \right\rfloor, \tag{3}$$

Now we have a multidimensional matrix $N_d(x,y)$, shown in Equation (4),

$$N_d(x,y) = \begin{pmatrix} p_{11d} & p_{12d} & & & p_{1Nd} \\ p_{21d} & p_{22d} & & & p_{2Nd} \\ \vdots & \vdots & \ddots & & \vdots \\ \vdots & \vdots & & \ddots & \vdots \\ p_{M1d} & p_{M2d} & & & p_{MNd} \end{pmatrix} \tag{4}$$

where M and N are the size of the processed image, and $d = 1, 2, 3, \ldots j$ 1 is the dimension of matrix N. Hence, the first dimension d represents the original image after it has been filtered by kernel of scale 2, and the second dimension represents the image filtered by kernel of scale 3, and so on until reaching the highest scale j.

Given $N_d(x,y)$ which represents the number of boxes necessary to cover the whole image, we perform the log operation on all elements $log(N_d(x,y))$ and the corresponding scaling factor $log(k)$. One of the advantages of the logarithm operation is that it expands the values of the dark pixels in the image while compressing the brighter values; also it compresses the dynamic range of images with large variations in pixel values. Finally, the fractal slope is determined from the least square linear regression line by computing the Sums of Squares as in (Fig. 3).

2.4. Volumes of interest selection

Since FD transformed images tend to be edge enhanced, all CT images were first transformed to a FD image to facilitate the processes of volume of interest (VOI) extraction. The VOIs for fractal analysis were the same VOIs as for the SUV_{max} and SUV_{avg}. (Fig. 4-a and -b) show a CT image before and after FD transformation, while (Fig. 4-c) is the windowed version with

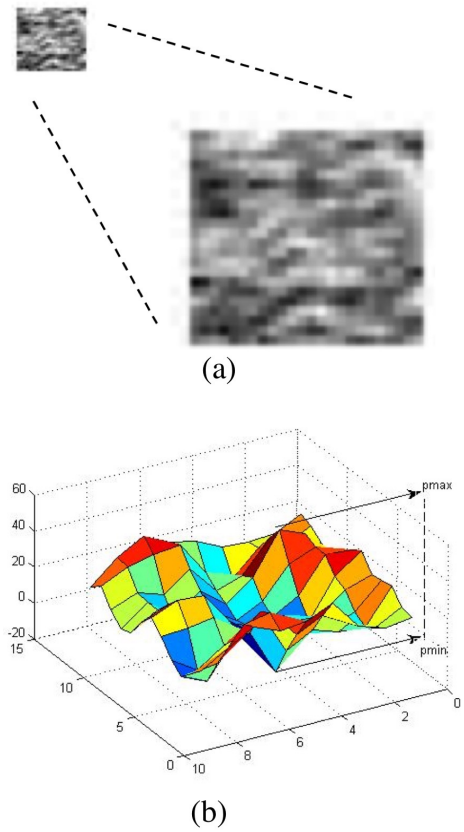

Figure 2: (a) Stage IB lung tumor volume of interest (VOI) enlarged to show texture, and (b) surface of corresponding VOI showing the maximum and minimum peaks in image texture intensity.

the window width and window grey level set in Hounsfield units for tumors as 300 HU and 48 HU, respectively. It is worth noting that tumors with sizes smaller than 1 cm – found in 2 cases – were excluded from the diagnostic statistics due to inherent noise resolution of CT, which render such analysis unreliable.

3. Results

The total FD values computed for all cases per stage and corresponding FDG are shown in Table 1, where the higher the larger the tumor size and more spread the higher the computed FD values. The FD was correlated with the corresponding maximum and average tumor ^{18}F-fluorodeoxyglucose

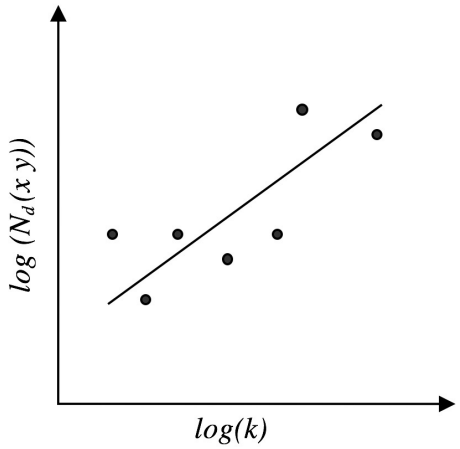

Figure 3: Estimating the fractal slope FD using least-squares linear regression in a log-log scale.

standardized uptake value (FDG-SUV) and tumor stage values measured by PET. It exhibited a medium Spearman Rank correlation (r) with good significance ($p < 0.005$) as shown in Table 2. Also, the fractal analysis of nodal (NI) and metastasis (MI) involvement are illustrated in (Fig. 5).

Table 1: Correlations and signi cant values for SUV_{avg}, SUV_{max}, and Stage versus FD

	r	p
SUV_{avg} vs FD	0.5732	0.0046
SUV_{max} vs FD	0.6294	0.0010
Stage vs FD	0.7831	<0.0001

A Mann-Whitney U test Pagano and Gauvreau [28] was applied to the FD for the lymph node involvement (NI) and the metastatic involvement (MI). Two groups were used NI = 0 i.e. node negative and node positive (i.e. NI = 1 to 3). Similarly, two groups were used for metastatic involvement, MI = 0 and MI = 1. The two tests showed good significance with $p < 0.05$ ($p_{NI} = 0.0139, p_{MI} = 0.0194$).

We empirically applied a threshold of FD > 1.955 to all cases and found that for those who had a CT of stage I or II had a higher likelihood of the NI and/or MI stage being upstaged by PET, Odds Ratio 5.38 (95% CI 0.99 -29.3). For those who are CT stage III or IV, and who have an FD below the

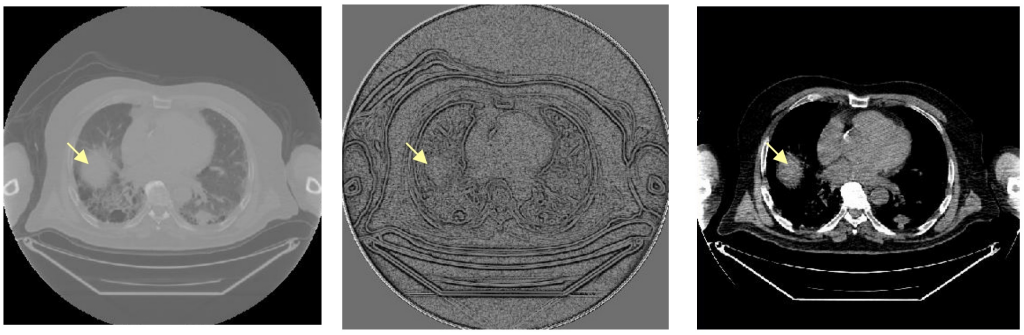

(a) (b) (c)

Figure 4: A CT image (a) before FD transformation, (b) after FD transformation, and (c) a windowed image after FD transformation.

Table 2: Lung tumor stage and corresponding average fractal dimension (FD_{avg}) values and ^{18}F- uorodeoxyglucose (SUV_{avg}) per stage

Stage	FD_{avg}		SUV_{avg}	
IA	1.91	0.28	4.03	1.67
IB	1.93	0.33	6.49	1.71
IIB	1.97	0.33	6.73	1.67
IIIA	2.02	0.30	6.37	0.92
IIIB	2.04	0.32	7.40	0.32
IV	2.04	0.30	5.63	0.55

same threshold they had an increased likelihood of the NI and/or MI stage being down staged by PET, Odds Ratio: 7.33 (95% CI 0.48 -111.2).

4. Discussion

Solid tumors of the lung usually have better contrast with the surrounding tissue than many other solid tumors, such as those found in abdominal and pelvic organs. This spatial information can be quantified by means of anatomical image texture analysis, which derives from the fact that different tissue types tend to have different properties. Investigating self-similarity of these texture variations at increasingly small scales, namely fractal analysis, can give indications on tumor heterogeneity in CT scans. Rather than merely focusing on measuring tumor size, attenuation and perfusion, fractal analysis can be considered as an additional non-invasive option to existing CT-based

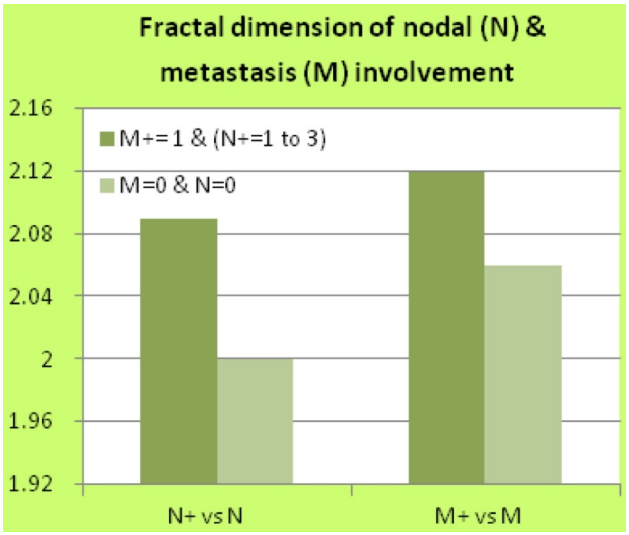

Figure 5: Higher fractal dimension (FD) values in CT images of NSCLC is associated with advanced stage and greater FDG uptake on PET.

imaging biomarkers.

This study examined the use of fractal analysis in CT images of non-small cell lung tumors. 56 CT images of lung tumors were analyzed and the maximum FDavg was correlated with the maximum and average FDG-SUV value and the nodal and metastatic stage. We found that the maximum FD had a medium correlation with good significance ($p < 0.005$) with the corresponding maximum and average FDG-SUV as determined by PET. Also when FD was correlated with lung tumor stage it was found to have good significance. Therefore, we propose that fractal analysis could be used as an index of tumor severity as we have shown that the FD value correlates with factors that describe tumor severity, the tumor stage and SUV.

Fractal analysis describes the complexity of a structure, the more complex the structure the higher the maximum FD value. In this paper we have looked at the relationship between fractal characteristics of texture and tumor stage, which is the first time that such work has been carried out for conventional non-contrast CT scans. We found that late stage tumors gave a higher FD value, therefore it seems that the more irregular a structure the higher stage it has. The association between the irregularity of a lesion and its aggression has been speculated on for many years. Siegelman et al looked at edge analysis of lesions on CT scans Siegelman et al. [29]. They classified the

margins of lesions as follows: 1, sharp and smooth; 2, moderately smooth; 3, some irregular undulations; and 4, grossly irregular with spiculations. 52 out of 66 nodules classified as 1 were benign, but 14 (21.2%) were malignant. 57.7% with type 2 edge were benign. 88.5% of type 3 and 4 edges were malignant. So their data indicated an association with irregular edge and malignancy. Peiss et al. Peiss et al. [30] investigated the usefulness of fractal analysis in the classification of lung tumors on chest radiographs. They found there was a clear separation between benign and malignant lesions with fractal distances of benign lesions being lower than those of malignant lesions. They argue that this was due to the more homogeneous structure of benign lesions. We assume that higher stage lesions are more irregular because they are more likely to be hypoxic and thus necrotic. Also higher stage lesions are more likely to have metastasized and in metastasis there is local invasion of tissues, spread into lymphatics or blood vessels by malignant cells and detachment this will undoubtedly give the tumor a more irregular appearance Fidler [31].

We also found that the maximum FD_{avg} had a good correlation with the FDG-SUV as determined by PET. Cancer cells have a high proliferation rate and have a higher glucose metabolism which means that FDG accumulates and the SUV value is an index of tumor accumulation. PET has been found to be more sensitive in detecting small volume disease with increased metabolic activity Lardinois [32]. This is extremely useful information as Eschmann et al found that the SUV can predict outcome in patients with advanced stage NSSLC and found it to be an independent factor, and also the incidence of distant metastases correlates with SUV average Eschmann et al. [33]. They also found that survival tended to decrease with increasing SUV_{avg}. Downey RJ et al also investigated whether SUVs predicted survival after lung cancer resection Downey et al. [34]. They found that the median maximal SUV is a predictor of overall survival after resection. The PLUS multicenter randomized trial looked at the effectiveness of PET in the preoperative assessment of patients with suspected NSCLC and found that the use of PET to stage patients prevented unnecessary surgery in one in five patients with suspected NSCLC van Tinteren et al. [35]. Therefore, the ability of FD to predict the likely SUV value will give extra information without the need for a PET scan.

Research has found that when PET is used to stage cancer it upstages most cancers but does down stage some. It is known overall that PET is better than conventional CT in the staging of lung cancer van Tinteren et al.

[35], Aukema et al. [36]. Lung cancer is said to be operable if the stage is IIIA or less and many patients have both a CT and PET to be confirm their stage. In clinical practice we propose that fractal analysis can be used to identify which patients are more likely to benefit from having a PET. We found that when the FD was calculated from non-contrast CT scans and a cut off value of 1.955 was applied, those above this threshold who had a CT stage of I or II were more likely to be upstage by the PET scan and those below this threshold with a CT stage of III or IV were more likely to be down staged.

If fractal analysis was used to select patients to go to PET scanning, this would impact on clinical management decisions. It provides extra information to physicians that could assist in making decisions earlier for appropriate candidates for surgery. Considering that up to 50% of curative surgery for suspected NSCLC is unsuccessful van Tinteren et al. [35], Aukema et al. [36], it would assist in stopping futile operations. The limitation of the study is that a relatively small number of images were analyzed, and a larger study with more lung tumors would exhibit a wider range of textures. Also, results of imaging studies can ultimately influence patient treatment and outcome, thus progress in radiomics-based test development needs to be grounded in sound scientific practice and be reproducible as well. Aspects involving practical reproducibility and replicability of computational data analysis methods needs to be considered. Such measures include investigating the self-similarity property of the proposed fractal analysis method on publicly available imaging databases, which can assist in ensuring replicability and generalizability of results.

5. Conclusion

The work indicates that higher FD in CT images of NSCLC is associated with advanced stage and greater FDG uptake on PET. Measurements of tumor FD on conventional CT examinations could potentially be used as a prognostic marker and/or to select patients for PET.

Performing fractal analysis in CT images of lung tumors can provide additional information about the likely tumor stage and likely FDG-SUV value, which will be used to determine the most appropriate treatment for patients with NSCLC. Also we propose that fractal analysis be used in clinical practice to select patients to go for PET who are likely to have their cancer stage altered by having a PET scan.

Acknowledgment

The author would like to thank the Clinical Imaging Science Center, Brighton, Sussex Medical School and Prof. Kenneth Miles (University College London) for the provision of medical data, and Dr. Elleny Panayiotou from Brighton & Sussex University Hospitals NHS Trust for useful discussions.

References

[1] T. Vos, C. Allen, M. Arora, R. M. Barber, Z. A. Bhutta, A. Brown, A. Carter, D. C. Casey, F. J. Charlson, A. Z. Chen, et al., Global, regional, and national incidence, prevalence, and years lived with disability for 310 diseases and injuries, 1990–2015: a systematic analysis for the global burden of disease study 2015, The Lancet 388 (2016) 1545–1602.

[2] Cancer Research UK, Lung cancer mortality statistics, Available from: `http://www.cancerresearchuk.org/cancer-info/cancerstats/types/lung/mortality/uk-lung-cancer-mortality-statistics`, 2018. [Online; accessed 22 Aug 2018].

[3] American Cancer Society, What are the key statistics about lung cancer?, Available from: `http://www.cancer.org/cancer/lungcancer-non-smallcell/detailedguide/non-small-cell-lung-cancer-key-statistics`, 2018. [Online; accessed 22 Aug 2018].

[4] C. Free, M. Ellis, L. Beggs, D. Beggs, S. Morgan, D. Baldwin, Lung cancer outcomes at a uk cancer unit between 1998–2001, Lung Cancer 57 (2007) 222–228.

[5] F. L. Greene, C. M. Balch, I. D. Fleming, A. Fritz, D. G. Haller, M. Morrow, D. L. Page, AJCC cancer staging handbook: TNM classification of malignant tumors, Springer Science & Business Media, 2002.

[6] N. C. C. for Cancer, et al., Lung cancer. the diagnosis and treatment of lung cancer, National Institute for Health and Clinical Excellence (2011).

[7] O. S. Al-Kadi, Tumour grading and discrimination based on class assignment and quantitative texture analysis techniques, Ph.D. thesis, University of Sussex, 2010.

[8] O. S. Al-Kadi, D. Watson, Texture analysis of aggressive and nonaggressive lung tumor ce ct images, IEEE transactions on biomedical engineering 55 (2008) 1822–1830.

[9] O. S. Al-Kadi, Assessment of texture measures susceptibility to noise in conventional and contrast enhanced computed tomography lung tumour images, Computerized medical imaging and graphics 34 (2010) 494–503.

[10] S. Kido, K. Kuriyama, M. Higashiyama, T. Kasugai, C. Kuroda, Fractal analysis of small peripheral pulmonary nodules in thin-section ct: evaluation of the lung-nodule interfaces, Journal of computer assisted tomography 26 (2002) 573–578.

[11] S. Kido, K. Kuriyama, M. Higashiyama, T. Kasugai, C. Kuroda, Fractal analysis of internal and peripheral textures of small peripheral bronchogenic carcinomas in thin-section computed tomography: comparison of bronchioloalveolar cell carcinomas with nonbronchioloalveolar cell carcinomas, Journal of computer assisted tomography 27 (2003) 56–61.

[12] B. Ganeshan, S. Abaleke, R. C. Young, C. R. Chatwin, K. A. Miles, Texture analysis of non-small cell lung cancer on unenhanced computed tomography: initial evidence for a relationship with tumour glucose metabolism and stage, Cancer imaging 10 (2010) 137.

[13] B. Ganeshan, E. Panayiotou, K. Burnand, S. Dizdarevic, K. Miles, Tumour heterogeneity in non-small cell lung carcinoma assessed by ct texture analysis: a potential marker of survival, European radiology 22 (2012) 796–802.

[14] G. R. Borst, J. S. Belderbos, R. Boellaard, E. F. Comans, K. De Jaeger, A. A. Lammertsma, J. V. Lebesque, Standardised fdg uptake: a prognostic factor for inoperable non-small cell lung cancer, European journal of cancer 41 (2005) 1533–1541.

[15] K.-H. Lee, S.-H. Lee, D.-W. Kim, W. J. Kang, J.-K. Chung, S.-A. Im, T.-Y. Kim, Y. W. Kim, Y.-J. Bang, D. S. Heo, High fluorodeoxyglucose

uptake on positron emission tomography in patients with advanced non–small cell lung cancer on platinum-based combination chemotherapy, Clinical cancer research 12 (2006) 4232–4236.

[16] M. P. Mac Manus, Z. Ding, A. Hogg, A. Herschtal, D. Binns, D. L. Ball, R. J. Hicks, Association between pulmonary uptake of fluorodeoxyglucose detected by positron emission tomography scanning after radiation therapy for non–small-cell lung cancer and radiation pneumonitis, International Journal of Radiation Oncology* Biology* Physics 80 (2011) 1365–1371.

[17] L.-F. de Geus-Oei, H. F. van der Heijden, E. P. Visser, R. Hermsen, B. A. van Hoorn, J. N. Timmer-Bonte, A. T. Willemsen, J. Pruim, F. H. Corstens, P. F. Krabbe, et al., Chemotherapy response evaluation with 18f-fdg pet in patients with non-small cell lung cancer, Journal of nuclear medicine 48 (2007) 1592–1598.

[18] Y. Ohno, H. Koyama, T. Yoshikawa, K. Matsumoto, N. Aoyama, Y. Onishi, K. Sugimura, Diffusion-weighted mri versus 18f-fdg pet/ct: performance as predictors of tumor treatment response and patient survival in patients with non–small cell lung cancer receiving chemoradiotherapy, American Journal of Roentgenology 198 (2012) 75–82.

[19] H.-q. Zhang, J.-m. Yu, X. Meng, J.-b. Yue, R. Feng, L. Ma, Prognostic value of serial [18f] fluorodeoxyglucose pet-ct uptake in stage iii patients with non-small cell lung cancer treated by concurrent chemoradiotherapy, European journal of radiology 77 (2011) 92–96.

[20] S. Chicklore, V. Goh, M. Siddique, A. Roy, P. K. Marsden, G. J. Cook, Quantifying tumour heterogeneity in 18 f-fdg pet/ct imaging by texture analysis, European journal of nuclear medicine and molecular imaging 40 (2013) 133–140.

[21] M. C. Adams, T. G. Turkington, J. M. Wilson, T. Z. Wong, A systematic review of the factors affecting accuracy of suv measurements, American Journal of Roentgenology 195 (2010) 310–320.

[22] O. S. Al-Kadi, Fractals for biomedical texture analysis, in: Biomedical Texture Analysis, Elsevier, 2017, pp. 131–161.

[23] B. B. Mandelbrot, The fractal geometry of nature, volume 173, WH freeman New York, 1983.

[24] J. Li, Q. Du, C. Sun, An improved box-counting method for image fractal dimension estimation, Pattern Recognition 42 (2009) 2460–2469.

[25] S. S. Chen, J. M. Keller, R. M. Crownover, On the calculation of fractal features from images, IEEE Transactions on Pattern Analysis and Machine Intelligence 15 (1993) 1087–1090.

[26] S. Buczkowski, S. Kyriacos, F. Nekka, L. Cartilier, The modified box-counting method: analysis of some characteristic parameters, Pattern Recognition 31 (1998) 411–418.

[27] N. Sarkar, B. B. Chaudhuri, An efficient differential box-counting approach to compute fractal dimension of image, IEEE Transactions on systems, man, and cybernetics 24 (1994) 115–120.

[28] M. Pagano, K. Gauvreau, Principles of biostatistics, CRC Press, 2018.

[29] S. S. Siegelman, N. Khouri, F. Leo, E. Fishman, R. Braverman, E. Zerhouni, Solitary pulmonary nodules: Ct assessment., Radiology 160 (1986) 307–312.

[30] J. Peiss, M. Verlande, W. Ameling, R. W. GÜNTHER, Classification of lung tumors on chest radiographs by fractal texture analysis, Investigative radiology 31 (1996) 625–629.

[31] I. J. Fidler, Tumor heterogeneity and the biology of cancer invasion and metastasis, Cancer research 38 (1978) 2651–2660.

[32] D. Lardinois, New horizons in staging for non–small-cell lung cancer, 2006.

[33] S. Eschmann, G. Friedel, F. Paulsen, M. Reimold, T. Hehr, W. Budach, J. Scheiderbauer, H. Machulla, H. Dittmann, R. Vonthein, et al., Is standardised 18 f-fdg uptake value an outcome predictor in patients with stage iii non-small cell lung cancer?, European journal of nuclear medicine and molecular imaging 33 (2006) 263–269.

[34] R. J. Downey, T. Akhurst, M. Gonen, A. Vincent, M. S. Bains, S. Larson, V. Rusch, Preoperative f-18 fluorodeoxyglucose-positron emission tomography maximal standardized uptake value predicts survival after lung cancer resection, Journal of Clinical Oncology 22 (2004) 3255–3260.

[35] H. van Tinteren, O. S. Hoekstra, E. F. Smit, J. H. van den Bergh, A. J. Schreurs, R. A. Stallaert, P. C. van Velthoven, E. F. Comans, F. W. Diepenhorst, P. Verboom, et al., Effectiveness of positron emission tomography in the preoperative assessment of patients with suspected non-small-cell lung cancer: the plus multicentre randomised trial, The Lancet 359 (2002) 1388–1392.

[36] T. S. Aukema, I. Kappers, R. A. V. Olmos, H. E. Codrington, H. van Tinteren, R. van Pel, H. M. Klomp, N. S. Group, et al., Is 18f-fdg pet/ct useful for the early prediction of histopathologic response to neoadjuvant erlotinib in patients with non–small cell lung cancer?, Journal of Nuclear Medicine 51 (2010) 1344–1348.